Seventh International Symposium on Nanotechnology in Construction (NICOM7)
Nanotechnology in Construction for Circular Economy
31 Oct - 2 Nov 2022

Advances in characterisation of carbonation behaviour in slag-based concrete using nanotomography techniques

B. Mehdizadeh [1*], K. Vessalas [2], B. Ben [3], A. Castel, S. Deilami [4], and H. Asadi [5]

[1] *PhD candidate, School of Engineering and Information Technology, University of Technology Sydney.*
[2] *Head of Discipline, Structural and Materials Engineering, Faculty of Engineering and Information Technology, University of Technology Sydney.*
[3] *Rigid Pavements Manager, Advanced Technical Services Infrastructure & Place, Transport for NSW.*
[4] *Professor, Technical Editor of Concrete in Australia, School of Civil and Environmental Engineering University of Technology Sydney*
[5] *Rigid Pavement Engineer, Advanced Technical Services Infrastructure & Place, Transport for NSW.*
[6] *Senior Manager (Pavements), Advanced Technical Services Infrastructure & Place, Transport for NSW*

[*] *Bahareh Mehdizadeh. Email: bahareh.mehdizadehmiyandehi@student.uts.edu.au*

ABSTRACT

Exposure of concrete to the surrounding atmosphere causes absorption of CO_2 and carbonation via a chemical reaction between the CO_2 and calcium hydroxide and calcium silicate hydrate reaction products that reside inside the concrete. A greater understanding of carbonation behaviour and its micro and nano-scale impact is needed to predict and model concrete durability, cracking potential and steel depassivation behaviours. New and sophisticated techniques have emerged to analyse the microstructural behaviour of concrete subjected to carbonation. High-resolution full-field X-ray imaging is providing new light for investigating nano-scale behaviour. Full-field nano-images provide significant insight into three-dimensional structural identification and mapping. Nanotomography modelling of an accelerated carbonated test specimen can also provide insight into the three-dimensional view of the pore structure that resides inside slag-based concrete. This is critical for better understanding the capillary porosity and pore solution behaviours of concrete in-situ. This paper investigates the durability properties, including the carbonation behaviour of slag-based concrete, by evaluating microstructural and nanotomography identification techniques.

Keywords: X-ray imaging, nanotomography, accelerated carbonated test, slag-based concrete

1. INTRODUCTION

Concrete is one of the most widely utilised construction materials in the world. The possibility of achieving high strength and durability has made concrete a well-established structural material for use in road, tunnelling and bridge infrastructure [1-4]. Various studies have been conducted to propose alternative materials to partially replace cement to reduce CO_2 emissions caused by cement production [5-8]. The utilisation of supplementary cementitious materials (SCMs) such as fly ash, slag, silica fume, etc. for partial replacement of cement are effective in making concrete more cost-effective, and high performing in terms of strength and durability requirements [9-16].

The carbonation of concrete caused by the presence of CO_2 in the atmosphere (approximately 380 ppm) acts as an environmental load and contributes a significant part of concrete structure deterioration [17]. This phenomenon is critical as it causes the alkalinity of the concrete to decrease (pH of 8). If the pH decreases below 12, the risk of corrosion is increased for any fixed steel components present within concrete elements [18, 19]. Carbonation can cause an increase in the porosity of concrete resulting in compressive strength and impermeability reduction in the carbonated zone of concrete. The results of several experimental studies reveal that the carbonation of slag-based concrete is highly dependent on the water/cement ratio, cement replacement ratio, curing methods, and in-situ environmental conditions [20-24]. Due to the nature of the carbonation process being long term in its manifestation, many researchers have used accelerated carbonation tests by adding pressurised CO_2 or increasing the temperature to increase the CO_2 diffusivity in the pore solution to shorten the experimental time [25–28].

Dependent on the cement replacement and the type of SCMs, the properties of SCM-based concrete change over time as a result of the hydration process and the carbonation behaviour [29-31]. After carbonation, the total capillary porosity volume of slag-based concretes increase. This can have a negative impact on the durability of the concrete by creating a larger pore structure, which is conducive to producing higher permeability coefficients for the concrete [32-34].

For controlling this behaviour, non-destructive techniques such as micro and nano tomography are often used to monitor a change in pore structure behaviour. These methods can be effective in investigating the progress of pore structure changes in slag-based concretes [35]. Han et al. [36] demonstrated how these modern technologies are useful to analyse concrete carbonation depth.

Recent advancements in micro and nano scale techniques give insight into forecasting and simulating concrete durability, cracking potential, and steel depassivation behaviours. This study identifies the main advances in micro and nano scale techniques in investigating carbonated concrete behaviour. Although several studies have been reviewed there is still limited information published about tomography techniques in better understanding carbonation behaviour of slag-based concretes.

2. Tomography Techniques

Tomography, in a broader sense, covers any techniques that employ sectional views as an intermediary stage before reassembling a three-dimensional object. This characterisation technique is useful in identifying the richness of the microstructure in three dimensions rather than only presenting two-dimensional projections. A three-dimensional micro and nano scale view is required to fully comprehend and monitor the behaviour in concrete. Materials scientists have used X-ray tomography techniques for decades to discover the behaviour of three-dimensional microstructures [36-40]. FIB/SEM tomography (focused-ion beam scanning electron microscopy), Electron tomography, X-ray micro-computed tomography (Micro-CT), and X-ray nano-computed tomography (Nano-CT) are non-destructive 3D imaging techniques useful for investigating the interior structures of a wide range of materials [34,35,38-41].

Tomography techniques can give new insights into concrete deterioration by providing precise information on the changed layers of concrete impacted by carbonation, corrosion, leaching, or sulphate attack [42]. Carbonation as a durability concern in concrete is a significant feature strongly influenced by microstructure and pore network characteristics. The porosity parameters obtained from the tomography data can successfully indicate the internal pore network geometry and microstructural features [37,43]. X-ray nano ad micro-computed techniques are useful techniques for monitoring slag-based concrete behaviour subjected to carbonation [44,45].

3. X-ray micro CT image methods:

X-ray micro-CT is a radiographic imaging technique that allows generating a series of cross-sectional images to identify the internal structure of materials without causing damage to the specimen [46-48]. In general, micro-CT can provide a series of reconstructed images represented by a pixel, either 8-bit or 16-bit. Micro-CT processing transforms 8 or 16-bit images into binary or segmented images, which are useful to examine the features of the specimen. A 3D microstructural image can be created by stacking 2D segmented images to analyse volumetric, multi-directional, and other advanced sample features. The pore structure of concrete can affect the qualities of the concrete, including strength, durability, and permeability. Using micro-CT images may help discover more information about these properties [49-52]. Although several scales are used such as macro-CT, micro-CT, and nano-CT, the spatial resolution of micro-CT can be used for microscopic CT scanning [46]. The micro-scale CT technique can scan a range from 1 cm to 10 µm in size, which is also a good range for investigating the size of capillary pores inside the cement paste [46,53-54]. For covering the whole range of cement paste pore size, nano-CT images can further scan a range of 10 µm to less than 10 nm in size [49,55]. To obtain high-quality nano-CT data necessitates meticulous sample preparation of a small size. Measuring 3D morphology for sizes less than 10 nm can give unique information on transportation characteristics and the mechanical and durability behaviour of concrete [56].

4. Carbonated concrete investigated using micro-CT and nano-CT

During the hydration process, cement paste interacts with CO_2. Carbonated cement paste can contribute to steel reinforcement corrosion and cause major and long-term durability issues for concrete structures. Several studies have noted that as carbonation develops, porosity reduces due to calcite formation filling the pore microstructure [57-60]. Phenolphthalein is a well-known technique for determining carbonation depth in concrete. However, this method necessitates the destruction of the sample, and the findings vary based on the sampling location [61,62]. Hence, X-ray micro and nano computed tomography (CT) as non-destructive techniques can identify and analyse the depth of carbonation and the microstructure of the concrete during the carbonation process [63-68]. Also, X-ray micro and nano CT scans can continually monitor the evolution of the carbonated areas of the same sample at different ages since it is a non-destructive testing technique [69].

Some researchers [70,71] have used micro-CT to determine the microstructural development of the cement paste during the carbonation process. Micro-CT images of cement paste are useful in finding the distribution of porosity and the effective pore width. In these aforementioned studies, the results of average porosities reveal that the porosity reduces following additional carbonation time. These infers that calcite (calcium bearing phase) has been formed during the carbonation process, and that porosity distribution may validate the pore microstructure change, e.g., reduction in porosity caused by carbonation. Since the porous structure of concrete extends from the nano to macroscopic scale [72], x-ray micro-CT and nano-CT with good resolutions are in high demand for characterising a wide range of behaviours [83]. Particle size and shape, interfacial topology, particle structure, pore structure, carbonation depth, and morphology of distinct solid phases in concrete have all been studied by these methods [73-77].

X-ray micro-CT results show that microcracks form from the surface to the inside of the cement paste after carbonation. Furthermore, the carbonated areas increase in depth with an increase in carbonation time. Moreover, cracks form during the carbonation process and reduce the density [78]. A new generation of laboratory-based nano-computed tomography (nano-CT) with high scale resolution has recently been introduced [46] for providing 3D images for measuring different properties of concrete like durability, cracking potential, and steel depassivation behaviours. Dimensional and transitional stability, is necessary for generating quality data with any instruments involved in sub-micron size imaging. Various applications demonstrate that nano-CT with spatially high resolution scanning is a well-established and mature method [79]. The porous and hierarchical structure of concrete extends from the macro to the nano-scale [80]. Nano-CT provides insight at the sub-micron scale. The ability to scan nano-CT in ambient settings keeps test samples in their natural form under normal and accelerated conditions [80-86]. Han et al. [86] revealed that by using nano-CT, the development of solid-phase composition, pore structure, damage degradation, and nano-mechanical characteristics of concrete, at different accelerated carbonation ages can be measured. The result of the aforementioned study reveals that without any prior drying preparation, X-ray computed tomography provides a suitable technique for obtaining 3D images of concrete in assessing the degree of microstructural damage.

5. Microstructural characteristics and properties of slag-based concrete during carbonation:

SCMs can play a critical role in controlling and improving the mechanical and durability properties of concrete [14-16]. Han et al. [86] described how micro-CT was utilised to track the progression of carbonation-induced fractures and how the carbonation depth increased with exposure duration for concrete containing a slag content up to 70% of total binder content. According to the micro-CT images shown in Fig.1 [83, 86], several cracks produced during the carbonation process can be seen. The appearance of these cracks indicate how micro-CT can be further utilised to categorise carbonation behaviour over time. The micro-CT results [86] reveal that the width and length of microcracks significantly impact the carbonation behaviour of concrete. More CO_2 penetration causes an increase in crack length. Meanwhile, when the fracture width is smaller than 10 µm at 1 year, CO_2 diffusivity around the crack is nearly equal to that in the surrounding concrete. However, when the fracture width exceeds 10 µm, the CO_2 diffusivity in concrete increases. When the crack width exceeds 100 µm, the CO_2 diffusivity is somewhat further increased [83,86-88].

In another study, Han et al. [68] analysed the carbonation depth of cement paste with different slag additions varying from 0% to 70% under 0 days to 14 days accelerated carbonation testing (after 3 months of curing). Because of slag's cementitious and pozzolanic properties, the hydration reaction of slag-based cement will improve the pore microstructure. Large pores will eventually transition into smaller pores with the pozzolanic reaction. This means the CO_2 diffusion coefficient will significantly decrease and therefore the rate of carbonation will also decrease. However, slag-based concrete generates a large amount of calcium hydroxide during the hydration process. Calcium hydroxide is an important chemical component in increasing the carbonation rate. The results from the Han et al. study demonstrated that the ideal slag addition amount to the binder to mitigate carbonation is no more than 50%. Fig.2 shows the specimen's carbonation front and depth of penetration with 50% and 70% slag during 14 days of accelerated carbonation. The carbonation front can be identified using micro-CT, which is seen to increase for 50% slag addition with the carbonation zone steadily expanding with an increase in curing time. However, for 70% slag addition, the specimens are observed to be totally carbonated in only 7 days. These findings demonstrate that the ideal slag addition, which mitigates carbonation, is less than 50%. Fig.3 shows the carbonation depth estimated from micro-CT appears to have the same result as the phenolphthalein method during 14 days of accelerated carbonation without the addition of slag. These results prove that micro-CT is a reliable and appropriate technique for characterising the carbonation depth of concrete [68]. Table 1 shows a summary of micro and nano-CT techniques and the test conditions of different samples in identifying carbonation behaviours.

Table 1. Use of micro and nano-CT for accelerated carbonation conditions.

	Type of Test	Sample or resolution	Test condition	w/c ratio
Ji-Su Kim [46]	6 weeks of the accelerated carbonation test.	resolution 65 µm Sample: 390 µm × 650µm × 520µm	temperature 20 ± 2 °C, relative humidity 60 ± 5% and 5% CO2 concentration	0.5
Dong Cui [71]	4 weeks of the accelerated test.	resolution 60 µm Sample: 9 mm × 40 mm × 40 mm	temperature 20 ± 2 C, relative humidity 70 ± 5% and 3% CO2 concentration	0.5
HAN Jiande [68]	14 weeks of the accelerated carbonation test.	0.066 mm × 0.066 mm × 0.066 mm	temperature 20 ± 2 C, relative humidity 70 ± 3% and 20% CO2 concentration	0.53
HAN Jiande [83]	12 weeks, 13 weeks, 14 weeks and 16 weeks of the accelerated carbonation test.	0.066 mm × 0.066 mm × 0.066 mm	temperature 20±2 C, relative humidity 75%±3%, CO2 concentration 20%±3%	0.53
Keshu Wan [89]	5 weeks and 6 weeks of the accelerated carbonation test.	pixel size of 60 µm.	temperature 20 ± 2 C, relative humidity of 70% ± 5%, CO2 concentration 20%	0.53

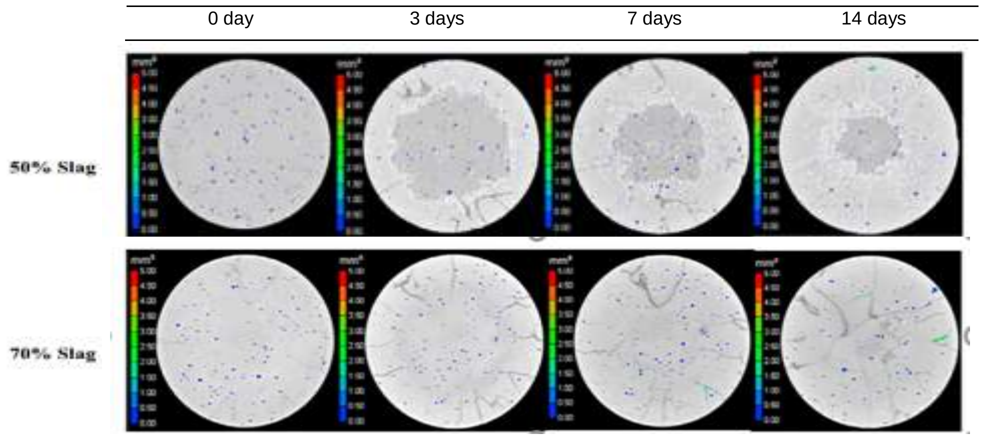

Fig.1 Cross-sectional images of the carbonation front for 50% and 70% slag with increasing accelerated carbonation testing times, 3D voxel size 0.086 mm^3. [68, 83]

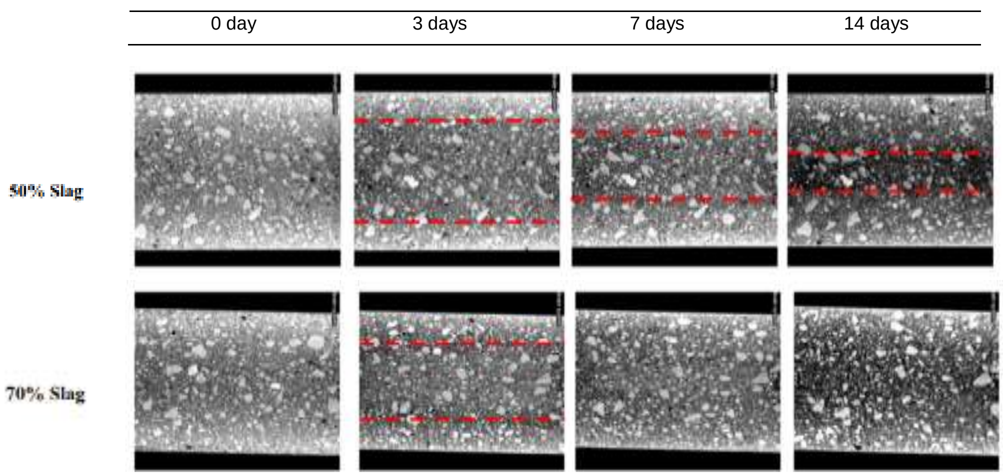

Fig. 2 View of the carbonation depth with 50% and 70% slag during 14 days of accelerated carbonation testing, 3D voxel size the 0.086 mm^3. [68]

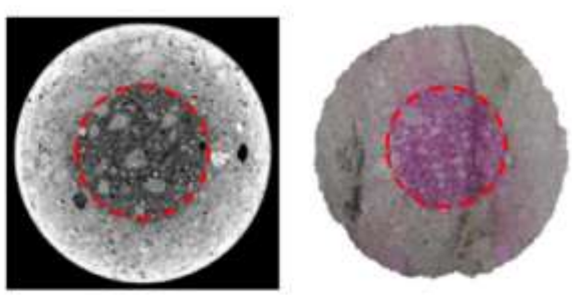

Fig. 3. Comparable images from the same results of micro-CT and phenolphthalein method for determining carbonation depth, 3D voxel size 0.086 mm^3. [68]

5. Conclusions

Tomography techniques for assessing carbonation behaviour in concrete are still in their early stage of development, but advances made in the previous decade have been significant. As has been demonstrated, micro and nano-CT methods efficiently and non-destructively investigate micro-structure and nano-structure behaviours. This technique is suitable for analysing micro and nano-scale topologies and morphologies, and studying the porosity network. The study outlines the advantages and benefits of using micro and nano X-ray CT to assess the pore network of concrete. Micro and nano CT 3-D imaging gives volumetric insight into the interactions between different phases and pores. The technique may be useful for characterising the carbonation behaviour of slag-based concretes for providing greater insight into an accelerated carbonation test and its impact on the pore structure. However, the need to employ small sample sizes necessitates meticulous sample preparations.

Acknowledgments

The authors gratefully acknowledged the University of Technology Sydney (UTS) and Transport for NSW (TfNSW) for providing the financial support required for this study.

References

[1] XG Li, Y. Lv, BG Ma, Q.B. Chen, X.B. Yin, S.W. Jian, Utilisation of municipal solid waste incineration bottom ash in blended cement, J. Clean. Prod. 32 (2012) 96e100.

[2] C. Chen, G. Habert, Y. Bouzidi, A. Jullien, Environmental impact of cement production: detail of the different processes and cement plant variability evaluation, J. Clean. Prod. 18 (5) (2010) 478–485, https://doi.org/10.1016/j. jclepro.2009.12.014.

[3] Glavind M. Sustainability of cement, concrete and cement replacement materials in construction. In: Khatib editor, Sustainability of Construction Materials. Wood Head Publishing in Materials. Cambridge, UK: Great Abington; 2009. p. 120 47.

[4] BM Miyandehi, A Feizbakhsh, MA Yazdi, Q Liu, J Yang, P Alipour, Combined effects of metakaolin, rice husk ash, and polypropylene fiber on the engineering properties and microstructure of mortar, Journal of Materials in Civil Engineering 29 (7), 04017025

[5] Flower D, Sanjayan J. Greenhouse gas emissions due to concrete manufacture. Int J Life Cycle Assess 2007; 12:282–8.

[6] Shariq M, Prasad J, Masood A. Effect of GGBFS on time dependent compressive strength of concrete[J]. Construction and Building Materials, 2010, 24(8): 1 469-1 478

[7] B Mehdizadeh, S Jahandari, K Vessalas, H Miraki, H Rasekh, B Samali, Fresh, mechanical, and durability properties of self-compacting mortar incorporating alumina nanoparticles and rice husk ash. Materials 14 (22), 6778.

[8] Mehrabi, P., Shariati, M., Kabirifar, K., Jarrah, M., Rasekh, H., Trung NT., Shariati, A., Jahandari, S., Effect of pumice powder and nano-clay on the strength and permeability of fiber-reinforced pervious concrete incorporating recycled concrete aggregate, Construction and Building Materials, 2021.

[9] Kazemi, M., Hajforoush, M., Khakpour Talebi, P., Daneshfar, M., Shokrgozar, A., Jahandari, S., Saberian, M., Li, J., 2020, In-situ strength estimation of polypropylene fibre reinforced recycled aggregate concrete using Schmidt rebound hammer and point load test, Journal of Sustainable Cement-Based Materials, 1-18.

[10] Jahandari, S., Saberian, M., Tao, Z., Faridfazel Mojtahedi, S., Li, J., Ghasemi, M., Rezvani, S.S., Li, W., 2019, Effects of saturation degrees, freezing thawing, and curing on geotechnical properties of lime and lime-cement concretes, Cold Regions Science and Technology. 160: 242–251.

[11] H, Rasekh., A, Joshaghani., S, Jahandari., F, Aslani., and M, Ghodrat., 2020. Rheology and workability of S.C.C. Woodhead Publishing Series in Civil and Structural Engineering, 31-63.

[12] E Mohseni, MA Yazdi, BM Miyandehi, M Zadshir, MM Ranjbar, Combined effects of metakaolin, rice husk ash, and polypropylene fiber on the engineering properties and microstructure of mortar, Journal of Materials in Civil Engineering 29 (7), 04017025

[13] Jung, Y.B.; Yang, K.H. Mixture-Proportioning Model for Low-CO2 Concrete Considering the Type and Addition Level of Supplementary Cementitious Materials. J. Korea Concr. Inst. 2015, 27, 427–434

[14] Australasian (iron & steel) Slag Association, "A Guide to the Use of Iron and Steel Slag in Roads", ISBN 0 9577051 58, Revision 2, 2002, Available from www. asa-inc.org.au, 27p.

[15] Building Research Establishment Digest 363, "Sulfate and acid resistance of concrete in the ground", 1996.

[16] SH Gh, Bahareh Mehdizadeh Miyandehi, M. M. Khotbehsara, M.Tarbiat" Study quality steel mill slag for use in concrete containing metakaolin", International Conference on advances in Engineering, 2015, Tehran, Iran.

[17] IPCC, Climate Change 2007 - The Fourth Assessment Report, Cambridge University Press, Cambridge, UK, 2007.

[18] N. Yoshida, Y. Matsunami, M. Nagayama, E. Sakai, Salt weathering in residential concrete foundations exposed to sulfate-bearing ground, J. Adv. Concr. Technol. 8 (2) (2010) 121–134.

[19] Elke, G.; van den Philip, H.; de Nele, B. Carbonation of slag concrete: Effect of the cement replacement level and curing on the carbonation coefficient—Effect of carbonation on the pore structure. Cem. Concr. Compos. 2013, 35, 39–48.

[20] Sisomphon, K.; Franke, L. Carbonation rates of concretes containing high volume of pozzolanic materials. Cem. Concr. Res. 2007, 37, 1647–1653.

[21] Monkman, S.; Shao, Y. Carbonation Curing of Slag-Cement Concrete for Binding CO2 and Improving Performance. J. Mater. Civ. Eng. 2010, 22, 296–304.

[22] Papadakis, V.G.; Tsimas, S. Effect of supplementary cementing materials on concrete resistance against carbonation and chloride ingress. Cem. Concr. Res. 2000, 30, 291–299.

[23] Demis, S.; Papadakis, V.G. A software-assisted comparative assessment of the effect of cement type on concrete carbonation and chloride ingress. Comput. Concr. 2012, 10, 391–407.

[24] M. Otieno, J. Ikotun, and Y. Ballim, "Experimental investigations on the effect of concrete quality, exposure conditions and duration of initial moist curing on carbonation rate in concretes exposed to urban, inland environment," Construction and Building Materials, vol. 246, Article ID 118443, 2020.

[25] L. Mo, F. Zhang, M. Deng, D.K. Panesar, Effectiveness of using CO2 pressure to enhance the carbonation of Portland cement-fly ash-MgO mortars, Cem. Concr. Compos. 70 (2016) 78–85, https://doi.org/10.1016/j.cemconcomp.2016.03.013.

[26] T. de Larrard, F. Benboudjema, J.B. Colliat, J.M. Torrenti, F. Deleruyelle, Concrete calcium leaching at variable temperature: experimental data and numerical model M.A.T. Marple et al. Cement and Concrete Research 156 (2022) 106760 12 inverse identification, Comput. Mater. Sci. 49 (2010) 35–45, https://doi.org/ 10.1016/j.commatsci.2010.04.017.

[27] L. Liu, J. Ha, T. Hashida, S. Teramura, Development of a CO2 solidification method for recycling autoclaved lightweight concrete waste, J. Mater. Sci. Lett. 20 (2001) 1791–1794.

[28] J.M. Bukowski, R.L. Berger, Reactivity and strength development of CO2 activated non-hydraulic calcium silicates, Cem. Concr. Res. 9 (1979) 57–68, https://doi.org/ 10.1016/0008-8846(79)90095-4.

[29] F. Matalkah, P. Soroushian, Carbon dioxide integration into alkali aluminosilicate cement particles for achievement of improved properties, J. Clean. Prod. 196 (2018) 1478–1485, https://doi.org/10.1016/j.jclepro.2018.06.186.

[30] X. Wang, K. Zhu, S. Ramli, L. Xu, F. Matalkah, P. Soroushian, A.M. Balachandra, Conversion of landfilled ash into hydraulic cements under different environments, Adv. Recycling Waste Manag. 2 (2017) 144, https://doi.org/10.4172/2475- 7675.1000144.

[31] K. Zhu, F. Matalkah, S. Ramli, B. Durkin, P. Soroushian, A.M. Balachandra, Carbon dioxide use in beneficiation of landfilled coal ash for hazardous waste immobilisation, J. Environ. Chem. Eng. 6 (2018) 2055–2062, https://doi.org/ 10.1016/j.jece.2018.03.003.

[32] B. Wu, G. Ye, Development of porosity of cement paste blended with supplementary cementitious materials after carbonation, Construction and Building Materials 145(2017), 52-61.

[33] Ye G, Experimental study and numerical simulation of the development of the microstructure and permeability of cementitious materials: TU Delft, Delft University of Technology; 2003

[34] GG Litvan, A Meyer, Carbonation of granulated blast furnace slag cement concrete during twenty years of field exposure , Special Publication, Symposium Paper, Volume: 91, 1445-1462, 1986 - concrete.org.

[35] Ahmed Sharif, Review on advances in nanoscale microscopy in cement research, micron, Elsevier, 80 (2016)45-58.

[36] J. Han, Y. Liang, W. Sun, W. Liu, S. Wang, "Microstructure modification of carbonated cement paste with six kinds of modern microscopic instruments", Journal of Materials in Civil Engineering2014, 27 (10) (Oct. 2015) 04014262, https://doi.org/10.1061/(ASCE)MT. 1943-5533.0001210.

[37] JL Provis, R.J. Myers, C.E. White, V. Rose, J.S.J. van Deventer, X-ray microtomography shows pore structure and tortuosity in alkali-activated binders, Cem. Concr. Res. 42 (2012) 855–864.
[38] De Rosier, D.J., Klug, A., 1968. Reconstruction of three-dimensional structures from electron micrographs. Nature 217 (5124), 130–134.
[39] Deshpande, A., Bao, W., Miao, F., Lau, C.N., LeRoy, B.J., 2009. Spatially resolved spectroscopy of monolayer graphene on SiO2. Physical Review B 79 (20), 205411.
[40] Frank, J., 2007. Electron Tomography: Three-dimensional Imaging with the Transmission Electron Microscope, 2nd ed. Plenum Press, New York.
[41] Cnudde, V., Boone, M.N., 2013. High-resolution X-ray computed tomography in geosciences: a review of the current technology and applications. Earth-Sci. Rev. 123, 1–17.
[42] H. Takahashi, T. Sugiyama, Investigation of alteration in deteriorated mortar due to water attack using non-destructive integrated CT-XRD method, in: K. Maekawa, A. Kasuga, J. Yamazaki (Eds.), Proceedings of the 11th fib International PhD Symposium in Civil Engineering, Tokyo, Japan, Aug. 2016, pp. 445–452.
[43] JL Provis, R.J. Myers, C.E. White, V. Rose, J.S.J. van Deventer, X-ray microtomography shows pore structure and tortuosity in alkali-activated binders, Cem. Concr. Res. 42 (2012) 855–864.
[44] R.R. Lloyd, J.L. Provis, JSJ van Deventer, Pore solution composition and alkali diffusion in inorganic polymer cement, Cem. Concr. Res. 40 (2010)
[45] L. Provis, Rupert J. Myers, Claire E. White, Volker Rose, Jannie S.J. van Deventer, X-ray microtomography shows pore structure and tortuosity in alkali-activated binders, John, Cement and Concrete Research, 42 (2012), 855-864.
[46] Sang-Yeop Chung, Ji-Su Kim, Dietmar Stephan , Tong-Seok Han, Overview of the use of micro-computed tomography (micro-CT) to investigate the relation between the material characteristics and properties of cement-based materials, Construction and Building Materials, 229(2019)116843.
[47] Anton du Plessis, William P. Boshoff y, A review of X-ray computed tomography of concrete and asphalt construction materials, Construction and Building Materials, 119(2019)637-651.
[48] K. Natesaiyer, C. Chan, S. Sinha-Ray, D. Song, C.L. Lin, J.D. Miller, E.J. Garboczi, A.M. Forster, X-ray CT imaging and finite element computations of the elastic properties of a rigid organic foam compared to experimental measurements: insights into foam variability, J. Mater. Sci. 50 (2015) 4012–4024.
[49] N. Bossa, P. Chaurand, J. Vicente, D. Borschneck, C. Levard, O.A. Chariol, J. Rose, Micro- and nano-X-ray computed-tomography: a step forward in the characterisation of the pore-network of a leached cement paste, Cem. Concr. Res. 67 (2015) 138–147.
[50] S.-Y. Chung, M.A. Elrahman, D. Stephan, P.H. Kamm, Investigation of characteristics and responses of insulating cement paste specimens with Aer solids using X-ray micro-computed tomography, Constr. Build. Mater. 118 (2016) 204–215.
[51] T.T. Nguyen, H.H. Bui, T.D. Ngo, G.D. Nguyen, Experimental and numerical investigation of influence of air-voids on the compressive behaviour of foamed concrete, Mater. Des. 130 (2017) 103–119.
[52] IB da Silva, X-ray computed microtomography technique applied for cementitious materials: a review, Micron 107 (2018) 1–8.
[53] E. Gallucci, K. Scrivener, A. Groso, M. Stampanoni, G. Margaritondo, 3D experimental investigation of the microstructure of cement pastes using synchrotron X-ray microtomography, Cem. Concr. Res. 37 (2007) 360–368.
[54] T.-S. Han, X. Zhang, J.-S. Kim, S.-Y. Chung, J.-H. Lim, C. Linder, Area of linealpath function for describing the pore microstructures of cement paste and their relations to the mechanical properties simulated from l-CT microstructures, Cem. Concr. Compos. 89 (2018) 1–17.
[55] S. Mindess, J.F. Young, D. Darwin, Concrete, second ed., Prentice Hall, New York, 2002.
[56] S. Brisard, R.S. Chae, I. Bihannic, L. Michot, P. Guttmann, J. Thieme, G. Schneider, P.J. Monteiro, P. Levitz, Morphological quantification of hierarchical geomaterials by X-ray nano-CT bridges the gap from nano to micro length scales, Am. Mineral. 97 (2-3) (2012) 480–483, https://doi.org/10.2138/am.2012.3985.
[57] V. Nagala, C. Page, Effect of carbonation on pore structure and diffusional properties of hydrated cement paste, Cem. Concr. Res. 27 (1997) 995–1007.
[58] B. Johannesson, P. Utgenannt, Microstructural changes caused by carbonation of cement mortar, Cem. Concr. Res. 31 (2001). 925 391.
[59] N. Li, N. Farzadnia, C. Shi, Microstructural changes in alkaliactivated slag mortars induced by accelerated carbonation, Cem. Concr. Res. 100 (2017) 214–226.
[60] D. Cui, W. Sun, N. Banthia, Use of tomography to understand the influence of preconditioning on carbonation tests in cement-based materials, Cem. Concr. Compos. 88 (2018) 52–63.
[61] J. Han, W. Sun, G. Pan, W. Caihui, Monitoring the evolution of accelerated carbonation of hardened cement pastes by Xray computed tomography, J. Mater. Civil Eng. 25 (3) (2012) 347-354.
[62] J. Han, W. Sun, G. Pan, Nondestructive microstructure analysis of the carbonation evolution process in hardened binder paste containing blast-furnace slag by X-ray CT, J. Wuhan Univ. Technique-Mater. Sci. Ed. 28 (5) (2013) 955- 962.

[63] J. Branch, R. Epps, D. Kosson, The impact of carbonation on bulk and itz porosity in microconcrete materials with fly ash replacement, Cem. Concr. Res. 103 (2018) 170–178.
[64] V. Papadakis, C. Vayenas, A reaction engginering approach to the problem of concrete carbonation, AlChE J. 35 (1989) 1639–1649
[65] A. Morandeau, M. Thiéry, P. Dangla, Investigation of the carbonation mechanism of CH and C-S-H in terms of kinetics, microstructure changes and moisture properties, Cem. Concr. Res. 56 (2014) 153–170.
[66] K. Wan, Q. Xu, Y. Wang, G. Pan, 3D spatial distribution of the calcium carbonate caused by carbonation of cement paste, Cem. Concr. Compos. 45 (2014) 255–263.
[67] M. Henry, I. Darma, T. Sugiyama, Analysis of the effect of heating and re-curing on the microstructure of high-strength concrete using X-ray CT, Constr. Build. Mater. 67 (2014) 37–46.
[68] J. Han, W. Liu, S. Wang, D. Du, F. Xu, W. Li, G. De Schetter, Effect of crack and ITZ and aggregate on carbonation penetration based on 3D micro X-ray CT microstructure evolution, Constr. Build. Mater. 128 (2016) 256–271.
[69] Weikang Konga, Ya Weia, Shuangjie Wang , Jianbing Chen , Yaqiong Wang, Research progress on cement-based materials by X-ray computed tomography, Chinese Society of Pavement Engineering, International Journal of Pavement Research and Technology Journal homepage: www.springer.com/42947.
[70] Effect of carbonation on cement paste microstructure characterised by micro-computed tomography, Ji-Su Kim, Kwang Soo Youm , Jae-Hong Lim , Tong-Seok Han, Construction and Building Materials 263(2020) 120079.
[71] Dong Cui, Wei Sun, Nemkumar Banthia, Use of tomography to understand the influence of preconditioning on carbonation tests in cement-based materials, Cement and Concrete Composites, 88(2018) 52-63.
[72] O. Coussy, Mechanics and Physics of Porous Solids, John Wiley & Sons Ltd, Chichester, United Kingdom, 2010.
[73] S. Brisard, C.A. Davy, L. Michot, D. Troadec, P. Levitz, Mesoscale pore structure of a high-performance concrete by coupling focused ion beam/scanning electron microscopy and small angle X-ray scattering, J. Am. Ceram. Soc. 102 (2019) 2905–2923.
[74] Y. Song, C.A. Davy, D. Troadec, X. Bourbon, Pore network of cement hydrates in a high performance concrete by 3D FIB/SEM — implications for macroscopic fluid transport, Cem. Concr. Res. 115 (2019) 308–326.
[75] Y. Song, J. Zhou, Z. Bian, G. Dai, Pore Structure Characterization of Hardened Cement Paste by Multiple Methods, Advances in Materials Science and Engineering, 2019.
[76] A. Sakdinawat and D. Attwood, Nanoscale X-ray imaging, nature Photonics, 4 (12) (2010), pp. 840-848.
[77] Rehbein, S., Heim, S., Guttmann, P., Werner, S., & Schneider, G. (2009). Ultrahigh-resolution soft-X-ray microscopy with zone plates in high orders of diffraction. Physical Review Letters, 103, 110801.
[78] HAN Jiande, SUN Wei, PAN Ganghua ,WANG Caihui , RONG Hui, Application of X-ray Computed Tomography in Characterization Microstructure Changes of Cement Pastes in Carbonation Process, 358, Vol.27 No.2.
[79] S. Bae, R. Taylor, D. Shapiro, P. Denes, J. Joseph, R. Celestre, S. Marchesini, H. Padmore, T. Tyliszczak, T. Warwick, D. Kilcoyne, P. Levitz, P.J. M Monteiro, Soft X-ray ptychographic imaging and morphological quantification of calcium silicate hydrates (C–S–H), J. Am. Ceram. Soc. 98 (12) (Dec. 2015) 4090–4095, https://doi.org/10.1111/jace.13808.
[80] S. Brisard, R.S. Chae, I. Bihannic, L. Michot, P. Guttmann, J. Thieme, G. Schneider, P.J. Monteiro, P. Levitz, Morphological quantification of hierarchical geomaterials by X-ray nano-CT bridges the gap from nano to micro length scales, Am. Mineral. 97 (2-3) (2012) 480–483, https://doi.org/10.2138/am.2012.3985.
[81] HAN Jiande et al: Application of X-ray Computed Tomography in Charact.
[82] Jun-zhe Liu , Ming-fang Ba , Yin-gang Du , Zhi-min He , Jian-bin Chen, Effects of chloride ions on carbonation rate of hardened cement paste by X-ray CT techniques, Construction and Building Materials, 112(2016) 619-627.
[83] J. Han, W. Sun, G. Pan, Analysis of different contents of blast-furnace slag effect on carbonation properties of hardened binder paste using micro-XCT technique in PRO83, Microstructural-related Durability of Cementitious Composites, RILEM Publications, 2012, pp. 228–234 ISBN: 978-2-35158-129-2, e-ISBN: 978-2-35158- 123-0.
[84] Brisarda, Marijana Serdarb , Paulo J.M. Monteiroc, Multiscale X-ray tomography of cementitious materials: A review Sébastien, Cement and Concrete Research, 128(2020)105824.
[85] O. Coussy, Mechanics and Physics of Porous Solids, John Wiley & Sons Ltd, Chichester, United Kingdom, 2010.
[86] HAN Jiande, SUN Wei, PAN Ganghua ,WANG Caihui , RONG Hui, Application of X-ray Computed Tomography in Characterization Microstructure Changes of Cement Pastes in Carbonation Process, 358, Vol.27 No.2 HAN Jiande et al: Application of X-ray Computed Tomography in Charact.
[87] Jun-zhe Liu , Ming-fang Ba , Yin-gang Du , Zhi-min He , Jian-bin Chen, Effects of chloride ions on carbonation rate of hardened cement paste by X-ray CT techniques, Construction and Building Materials, 112(2016) 619-627.
[88] Bushby, A.J., P'ng, K.M., Young, R.D., Pinali, C., Knupp, C., Quantock, AJ, 2011. Imaging three-dimensional tissue architectures by focused ion beam scanning electron microscopy. Nat. Protoc. 6 (6), 845–858.
[89] Keshu Wan , Qiong Xu , Yudong Wang , Ganghua Pan, 3D spatial distribution of the calcium carbonate caused by carbonation of cement paste, Cement & Concrete Composites, 45(2014)255-263.